21cm Cosmology

Foreground Challenges

Abhirup Datta

Center of Astronomy
Indian Institute of Technology Indore
&
Center for Astrophysics & Space Astronomy
University of Colorado Boulder

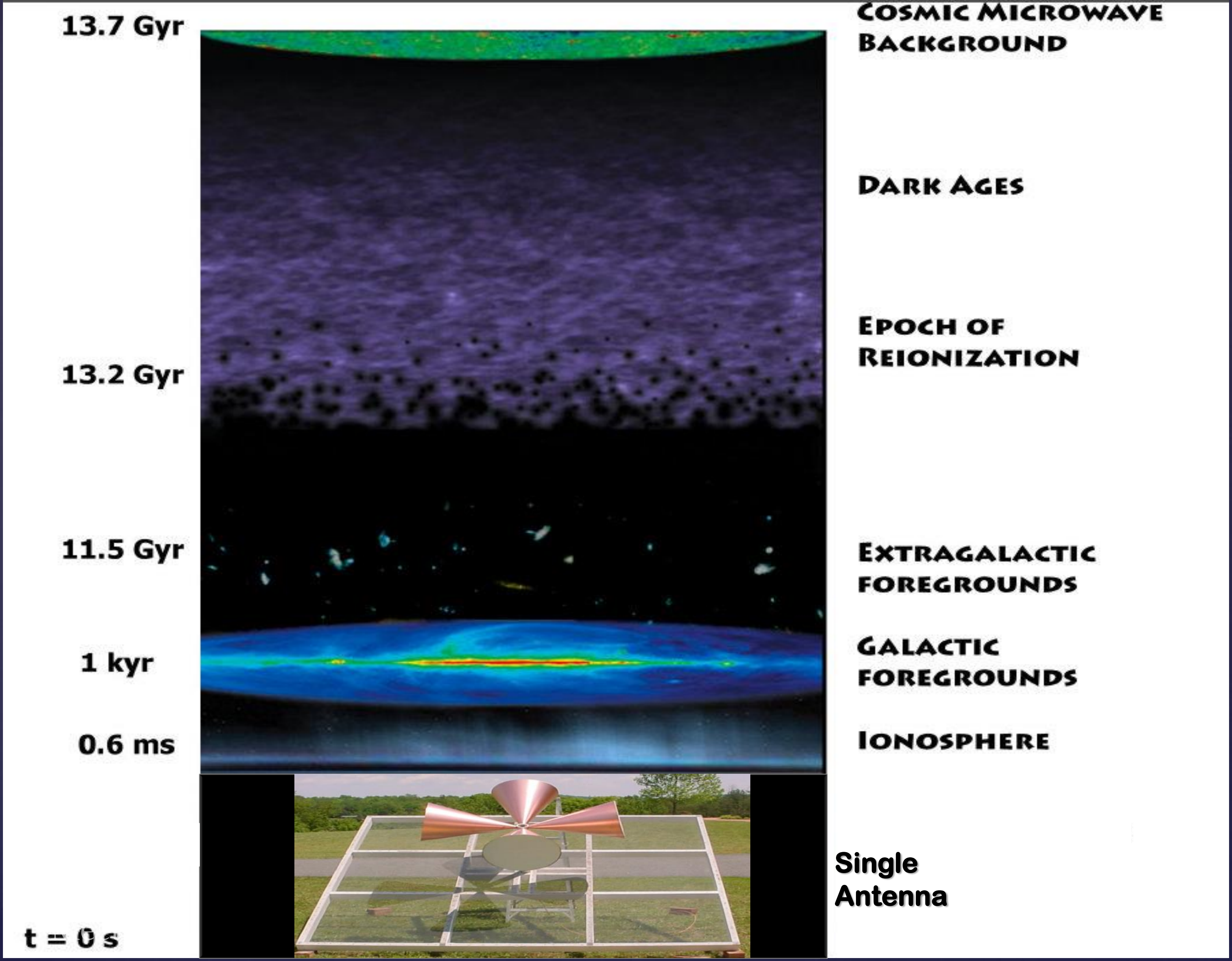

Diagram has been modified from a LOFAR presentation by S. Zaroubi (http://www.lsw.uni-heidelberg.de/users/christlieb/teaching/WS0910/100126_Zaroubi_LOFAR.pdf)

Extraterrestrial Foregrounds

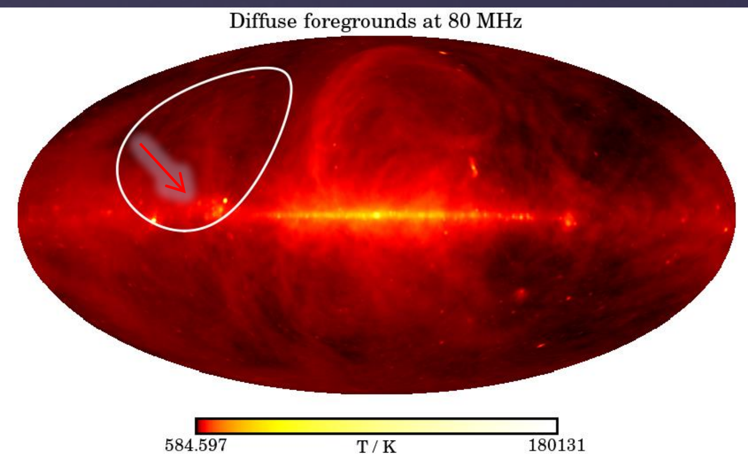

$$\sigma(\nu) = \frac{T_{sys}(\nu)}{\sqrt{\delta\nu * \delta t}}$$

Thermal Noise 2 mK in 100 Hours, 0.5 MHz @ 60 MHz

Spectra of Foregrounds

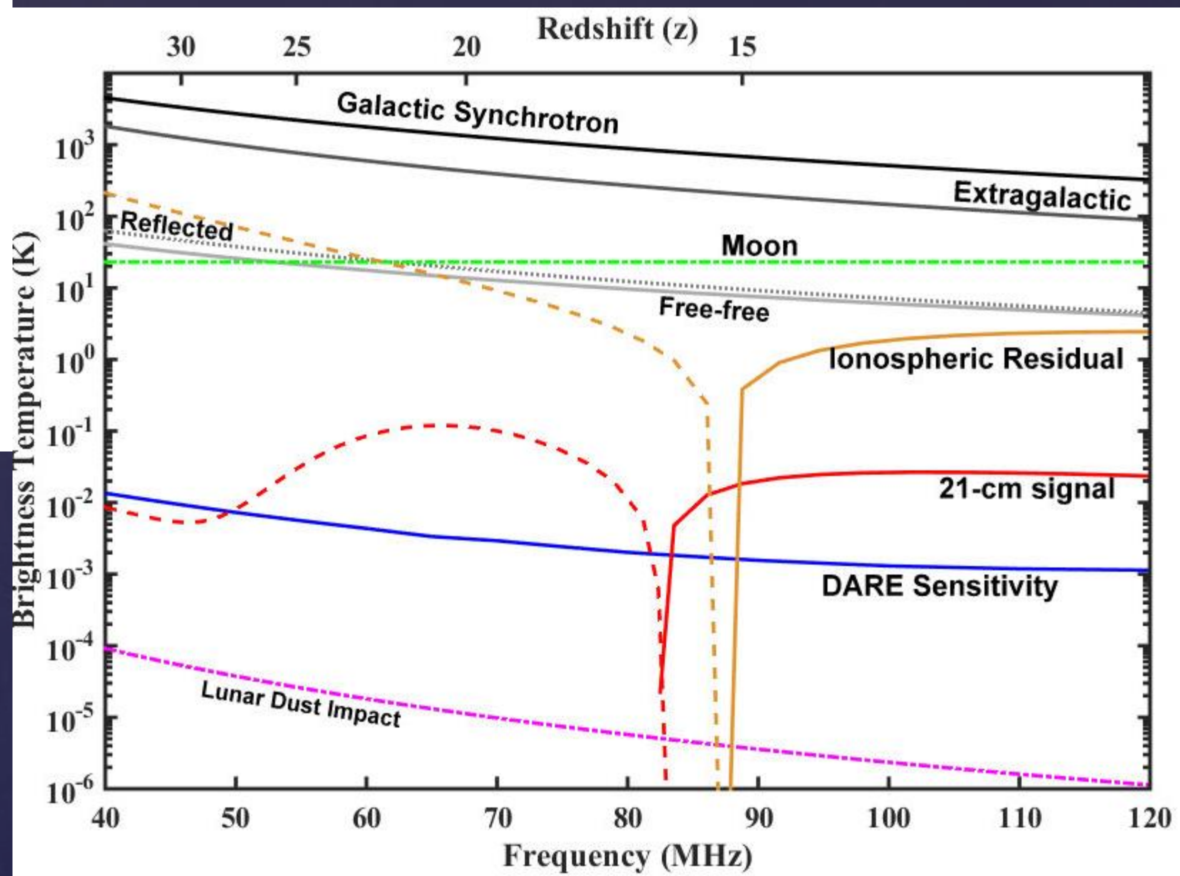

Current/Upcoming Global Signal Experiments

Experiment	Site	ν range (MHz)
EDGES	WA	100-200
DARE	Moon	40-120
LEDA	NM	30-80
DAWN	NM	30-80
BigHorns	WA	50-200
SARAS	India	87.5-175

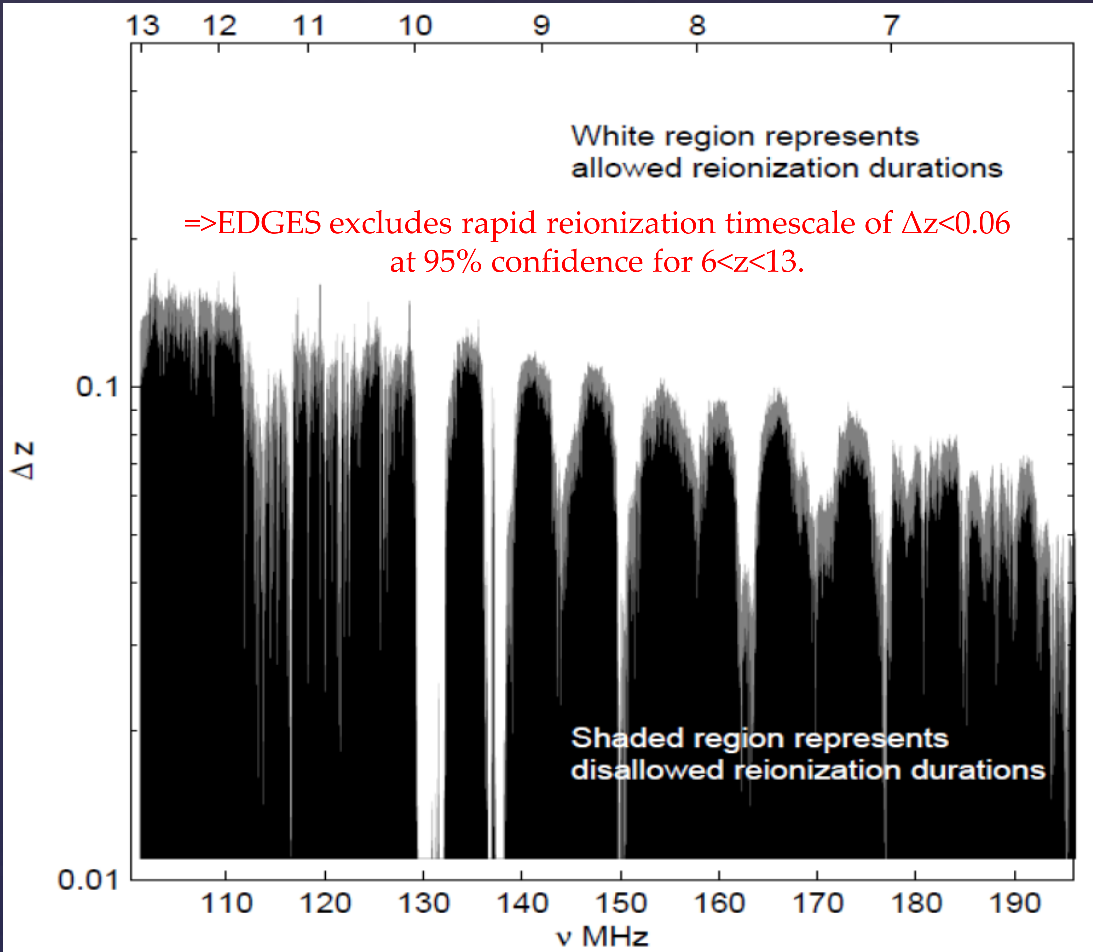

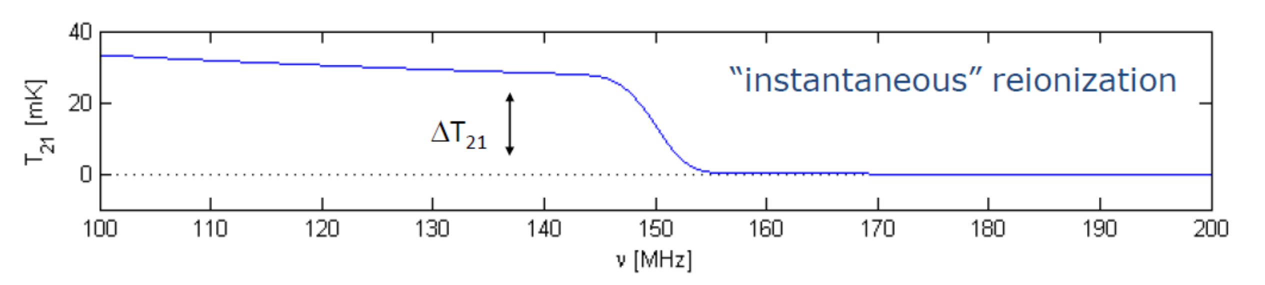

Foreground Removal Methods

Hierarchically removing foreground from data based on previous knowledge of the nature of the foreground	Simultaneously fitting for both Foreground and Signal Parameters
Bowman et al. 2008, 2010.	Harker et al. 2012
Rogers et al. 2008, 2012.	Harker 2015
Voytek et al. 2013	Harker et al. 2015
Bernardi et al. 2013	Mirocha et al. 2015

Either schemes rely on the accurate knowledge of the nature of the foreground- Otherwise the signal recovery becomes a **challenge**!

HI Fluctuations
Current and Future Experiments

Experiment	Site	Type	ν (MHz)	Goal
GMRT	India	Parabola array	150-200	CSS/PS
MWA	Australia	Aperture array	80-240	PS
LOFAR	Netherlands	Aperture array	115-240	PS/CSS
PAPER/HERA	South Africa	Dipole Array	110-190	PS/CSS
SKA	Australia	Aperture array	70-240	Imaging

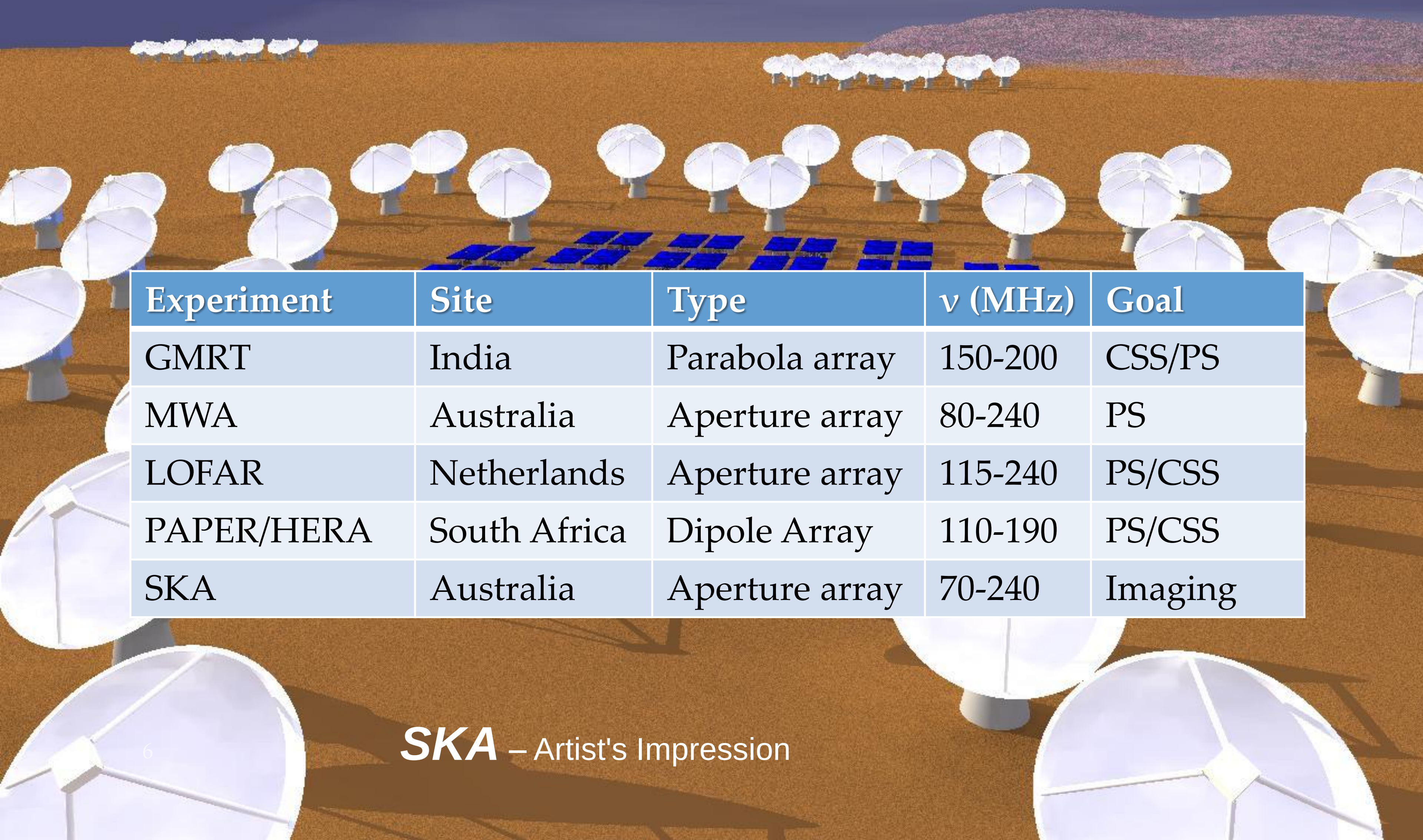

SKA – Artist's Impression

Foreground Removal Methods

Foreground Avoidance	Foreground suppression	Foreground Removal
Datta et al . 2010 Trott et al. 2012 Morales et al. 2012 Parsons et al. 2013 Pober et al. 2013 Liu et al. 2014a,b	TGE - Choudhury et al. 2014, 2016 CHIPS - Trott et al. 2015 HIEMICA - Zhang et al. 2015	Liu et al. 2008 Datta et al. 2009 WP smoothing - Harker et al. 2008, 2010 FASTICA – Chapman et al. 2013 GMCA - Chapman et al. 2012, 2016

Either schemes rely on the accurate knowledge of the nature of the foreground at different scales- Otherwise the signal recovery becomes a **challenge**!

Foreground Removal

1. Parametric Methods

a. Polynomial Fitting : $\log T_{b,\, fg}\,(\nu) = a_0 + \sum a_i \;\log \nu_i$

McQuinn et al. (2006); Morales et al. (2006); Gleser et al. (2008); Jelic et al. (2008); Bowman et al. (2006); Liu et al. (2009); Datta et al. (2009); Petrovic & Oh (2011)

b. CCA (Correlated Component Analysis) – Bonaldi & Brown (2015)

- Foreground subtraction step compensates for small errors in the parametric model adopted by the CCA, which result in a slight over/underestimation of the amplitude of the foregrounds at a given frequency.

Foreground Removal

1. Non- Parametric Methods

a. Wp smoothing: Harker et al. 2009

b. GMCA (Generalized Morphological Component Analysis) – Chapman et al. 2012, 2013

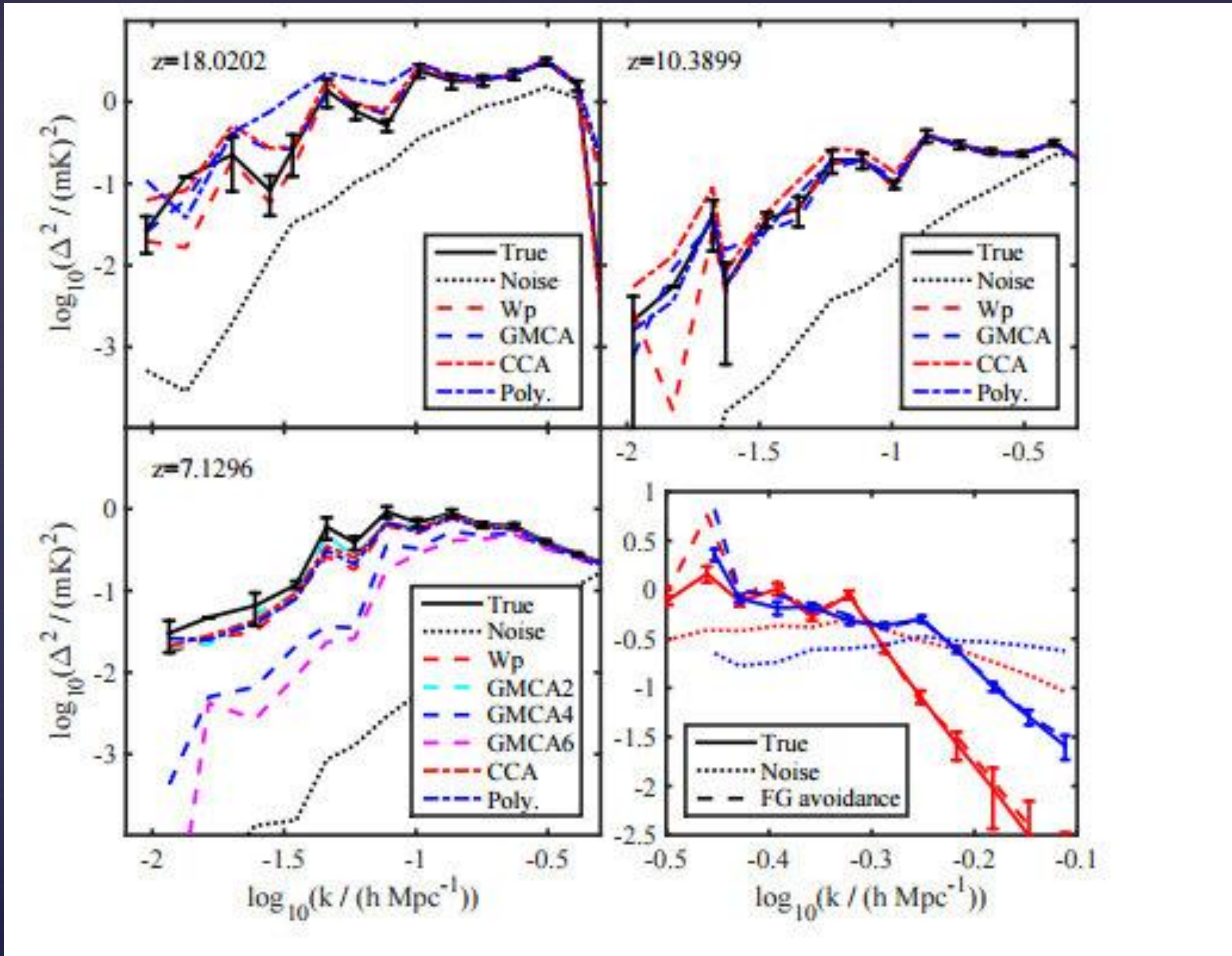

Chapman et al. 2015

Power Spectra Analysis:

Datta et al. 2010

- 1D Spherically-Averaged power Spectra P(k):

$$P(\tilde{\mathbf{k}}) = \frac{\sum_{|\mathbf{k}|=\tilde{\mathbf{k}}} W_u(\mathbf{k})\,|V(\mathbf{k})|^2}{\sum_{|\mathbf{k}|=\tilde{\mathbf{k}}} W_u(\mathbf{k})}$$

- 2D Power Spectra P(kperp,kpar):

$$P\left(\tilde{k_\perp}, \tilde{k_\parallel}\right) = \frac{\sum_{|\mathbf{k}_\perp|=\tilde{k_\perp}} \sum_{|k_\parallel|=\tilde{k_\parallel}} W_u(k_\perp, k_\parallel)\left|V(k_\perp, k_\parallel)\right|^2}{\sum_{|\mathbf{k}_\perp|=\tilde{k_\perp}} \sum_{|k_\parallel|=\tilde{k_\parallel}} W_u(k_\perp, k_\parallel)}$$

Observed Coordinates	$(\boldsymbol{\theta}_\mathbf{x}, \boldsymbol{\theta}_\mathbf{y})$	F.T. →	$(\mathbf{k}_\mathbf{x}, \mathbf{k}_\mathbf{y}) \equiv \mathbf{k}_{perp}$	Power spectrum
In the image of the sky	$\boldsymbol{\nu}$ --> redshift	F.T. →	$\mathbf{k}_\mathbf{z} \equiv \mathbf{k}_{par}$	Coordinates

2D Power Spectra – EoR Window

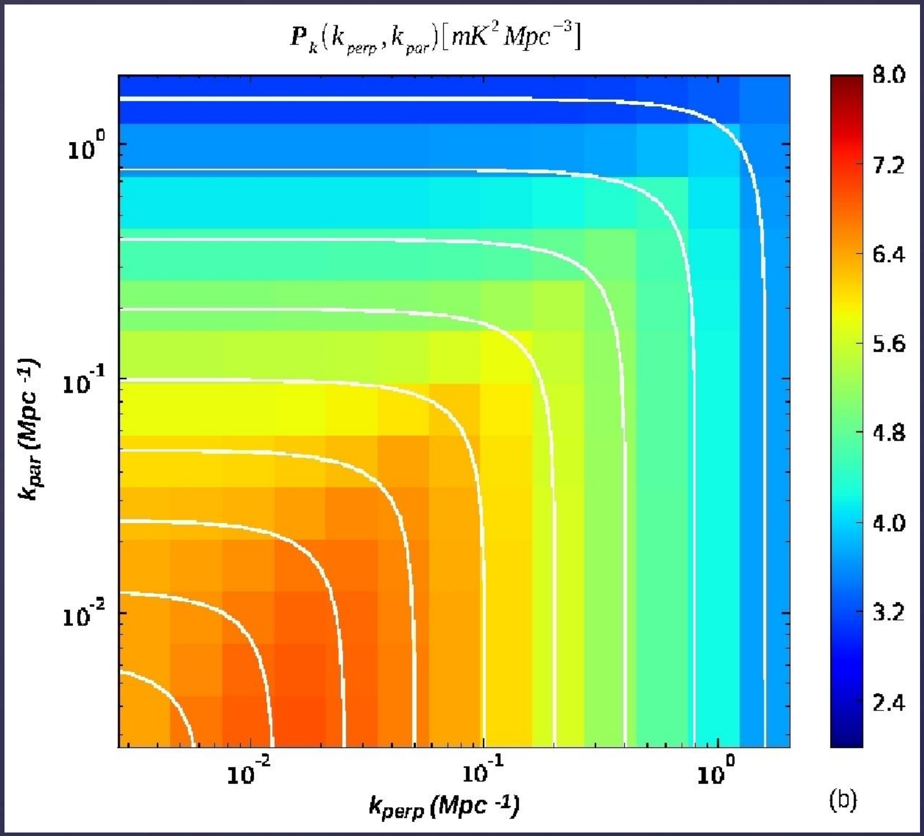

HI 21cm signal PS

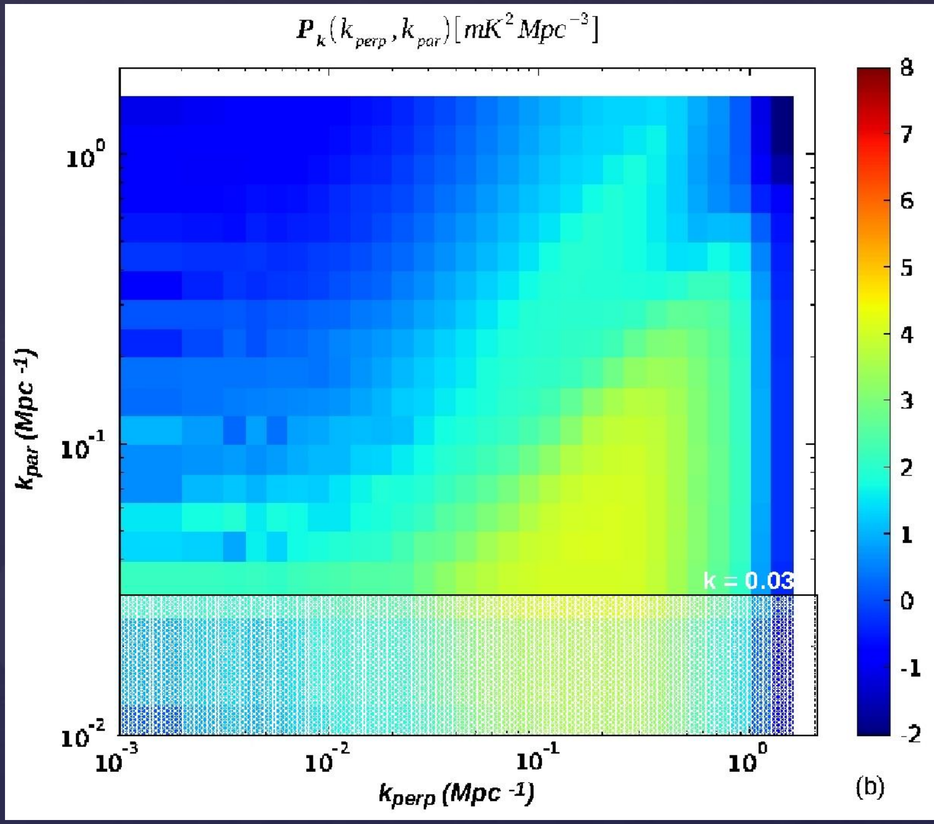

Residuals after GSM+polynomial subtraction

Contributions are decoupled along two axes

Errors localized at higher K values > 0.05

Signal dominates over residuals at K_{par} ~ 0.1

Datta et al. 2010

2D Power Spectra – EoR Window

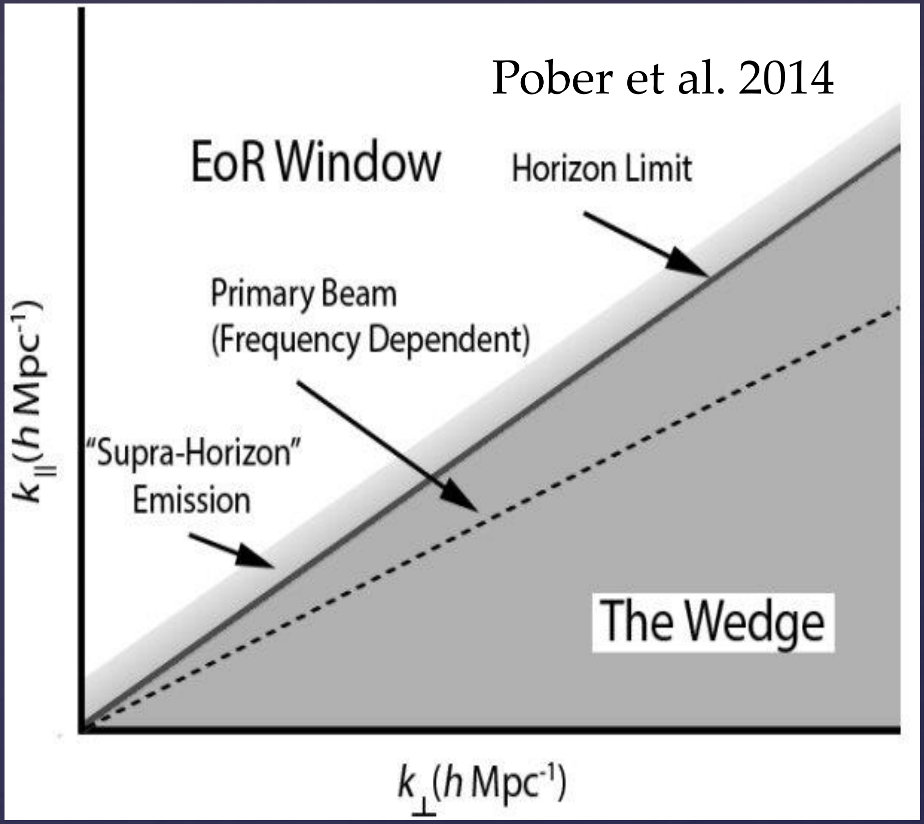

Wedge Geometry - explained

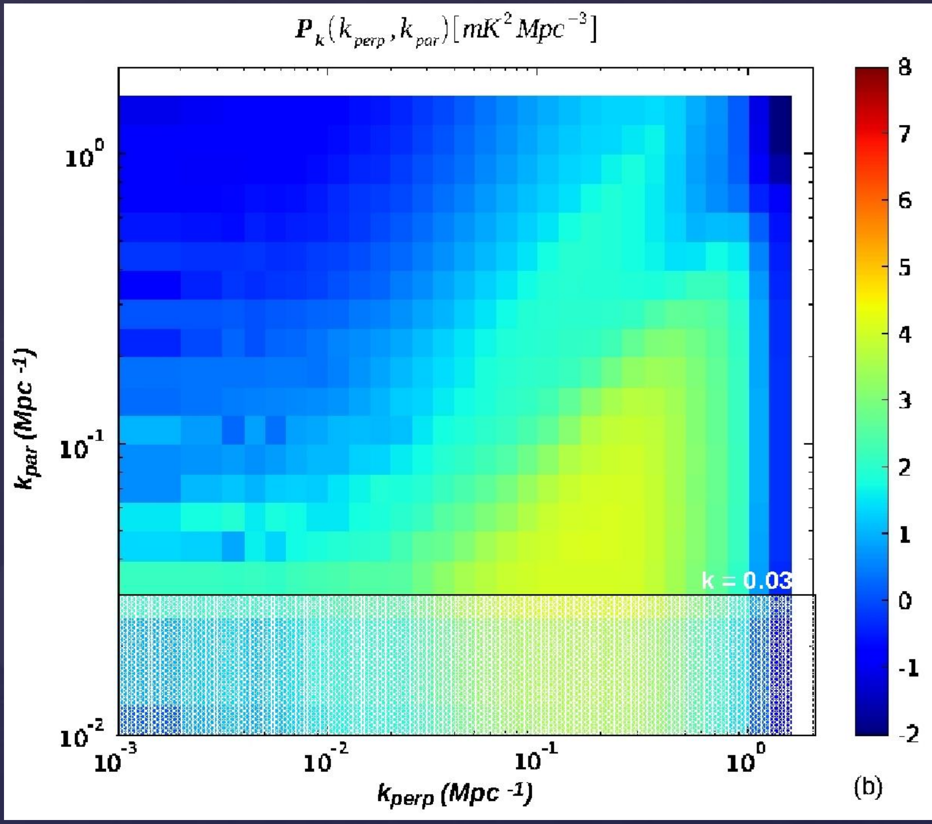

Residuals after GSM+polynomial subtraction

Contributions are decoupled along two axes

Errors localized at higher K values > 0.05

Signal dominates over residuals at $K_{par} \sim 0.1$

Datta et al. 2010

Low–Frequency Foregrounds at 408 MHz

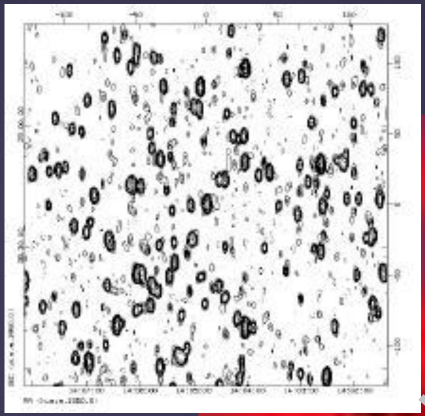

Effelsberg 408 MHz Image
(Haslam + 1982)

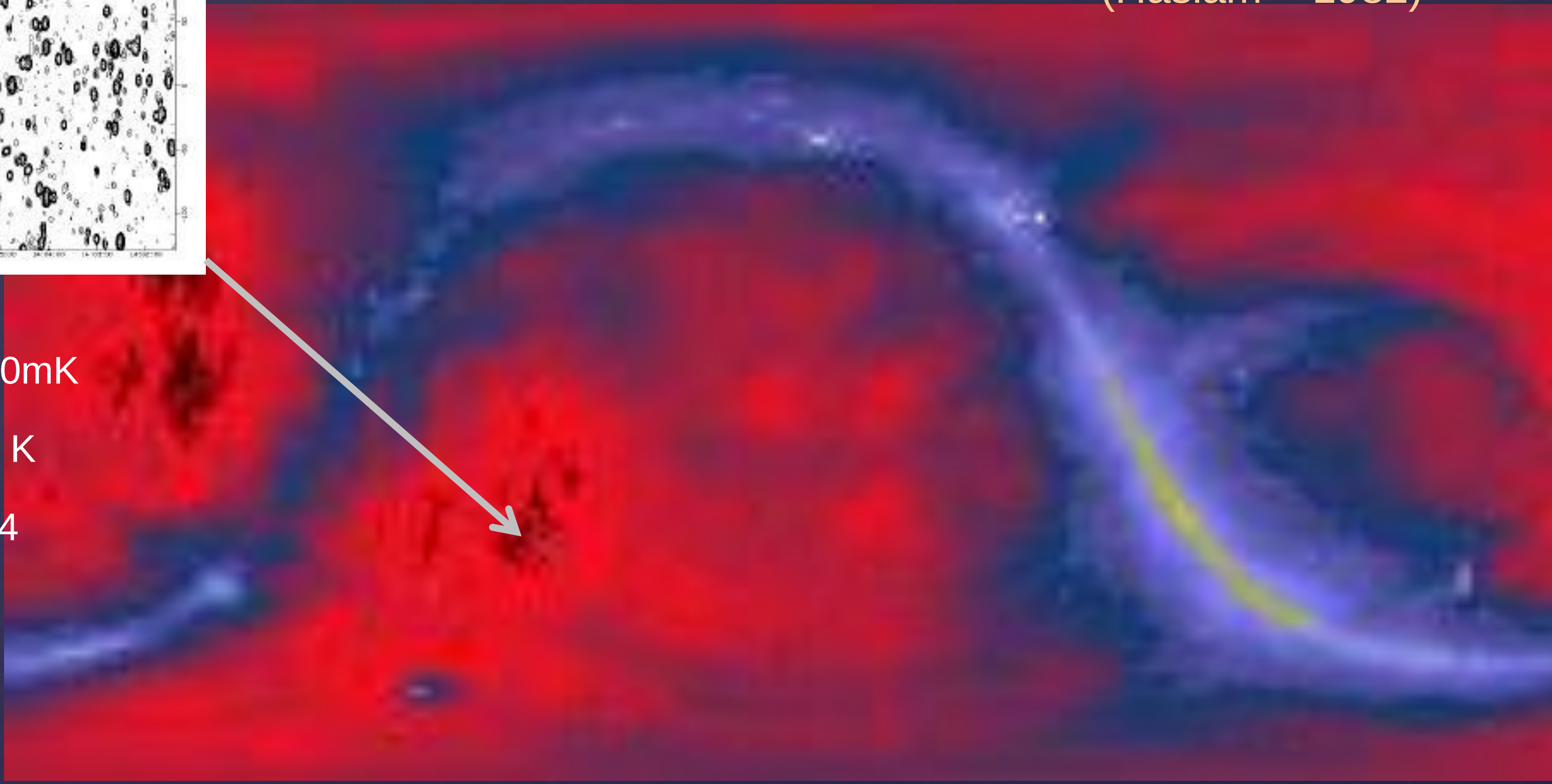

Signal < 20mK

Sky > 200 K

DNR > 1e4

- Coldest regions: T ~ 180 $(\nu/180\ \mathrm{MHz})^{-2.6}$ K
- 90% = Galactic foreground (~200-1000K, 99% Synchrtron, 1% Free-free),
10% = Egal. radio sources (~50K) , Galactic RRLs (< 1K), Sun

Low–Frequency Foregrounds at 45 MHz

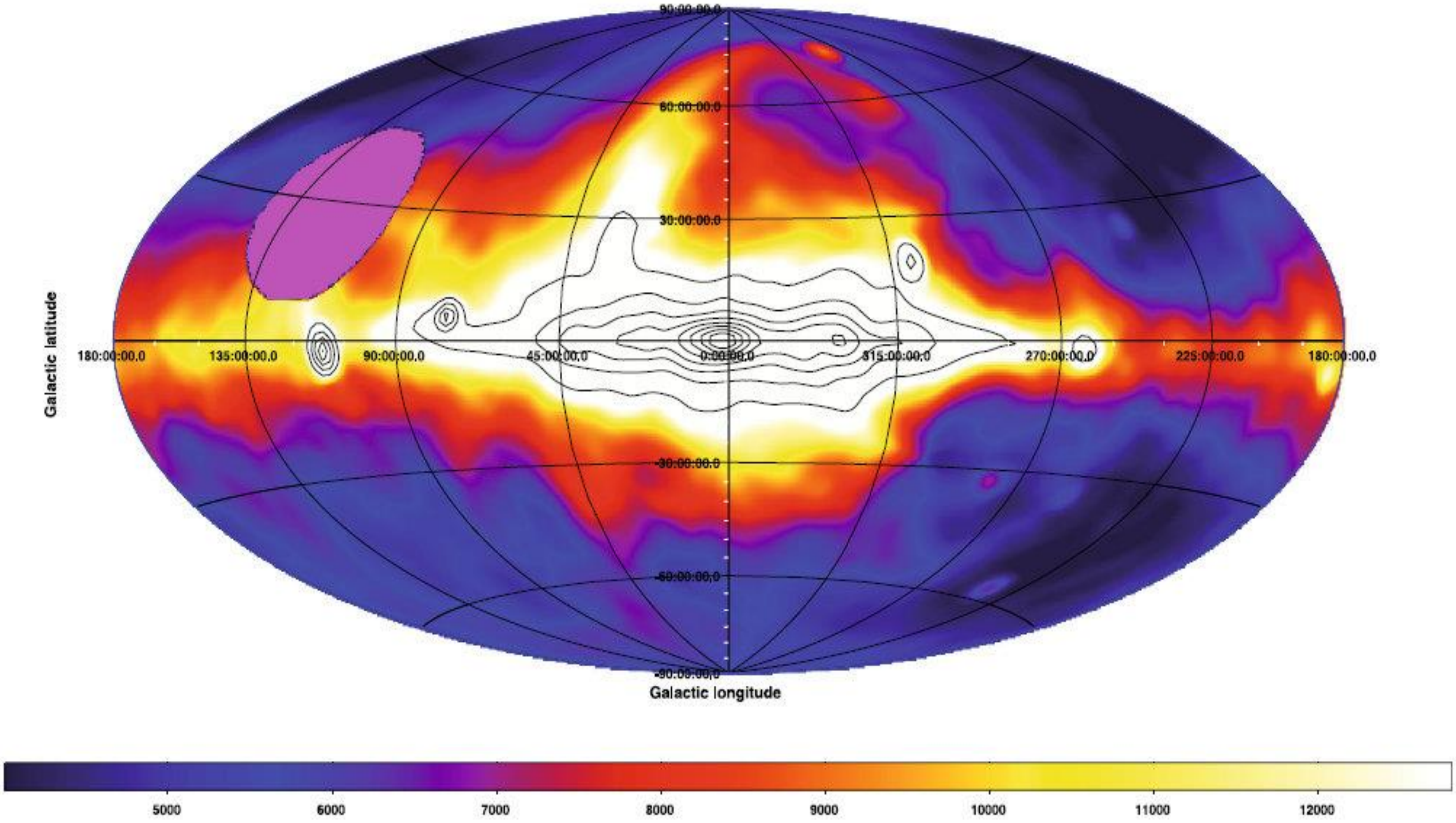

Maipu and MUradar

Guzman et al. 2011

Project/Instrument	ν(GHz)	Area	Resolution	Ref.
DRAO, CAN	0.01	N	$2.6 \times 1.9°$	Caswell (1976)
DRAO, CAN	0.022	N	$1.1 \times 1.7°$	Roger et al. (1999)
MRAO+JMUAR	0.045	F	$\sim 3.6°$	Alvarez et al. (1997); Maeda et al. (1999)
Parkes	0.085	E	$3.8 \times 3.5°$	Landecker & Wielebinski (1970)
Parkes	0.15	E	$2.2°$	Landecker & Wielebinski (1970)
GER, AUS, ENG	0.408	F	$48'$	Haslam et al. (1981, 1982); Remazeilles et al. (2015)
Dwingeloo, NLD	0.82	N	$1.2°$	Berkhuijsen (1971)
CHIPASS	1.39	S	$14.4'$	Calabretta et al. (2014)
Stokert, Villa Elisa	1.42	F	$36'$	Reich (1982); Reich & Reich (1986); Reich et al. (2001)
Rhodes/HartRAO	2.33	S	$20'$	Jonas et al. (1998)
WMAP	22.8	F	$49'$	Hinshaw et al. (2009)
Planck	30	F	$32'$	Planck Collaboration et al. (2015)
WMAP	33	F	$37'$	Hinshaw et al. (2009)
WMAP	40.7	F	$29'$	Hinshaw et al. (2009)
Planck	44	F	$24'$	Planck Collaboration et al. (2015)
WMAP	60.8	F	$20'$	Hinshaw et al. (2009)
Planck	70	F	$14'$	Planck Collaboration et al. (2015)
WMAP	93.5	F	$13'$	Hinshaw et al. (2009)
Planck	100	F	$10'$	Planck Collaboration et al. (2015)
Planck	143	F	$7'$	Planck Collaboration et al. (2015)
Planck	217	F	$5'$	Planck Collaboration et al. (2015)
Planck	353	F	$5'$	Planck Collaboration et al. (2015)
Planck	545	F	$5'$	Planck Collaboration et al. (2015)
Planck	857	F	$5'$	Planck Collaboration et al. (2015)
AKARI	1875	P	$1.5'$	Doi et al. (2015)
AKARI	2143	P	$1.5'$	Doi et al. (2015)
IRAS (IRIS)	3000	F	$4.3'$	Miville-Deschênes & Lagache (2005)
AKARI	3333	P	$1.5'$	Doi et al. (2015)
IRAS (IRIS)	5000	P	$4'$	Miville-Deschênes & Lagache (2005)

Table 1. List of sky maps we use in our multi-frequency modeling. F: full sky; S: southern sky; N: northern sky; E: equatorial plane; P: partial sky. CHIPASS at 1.39 GHz has a bandwidth of 64 MHz, so its frequency largely overlaps with the Stokert+Villa Elisa map at 1.42 GHz.

Zheng et al. 2016

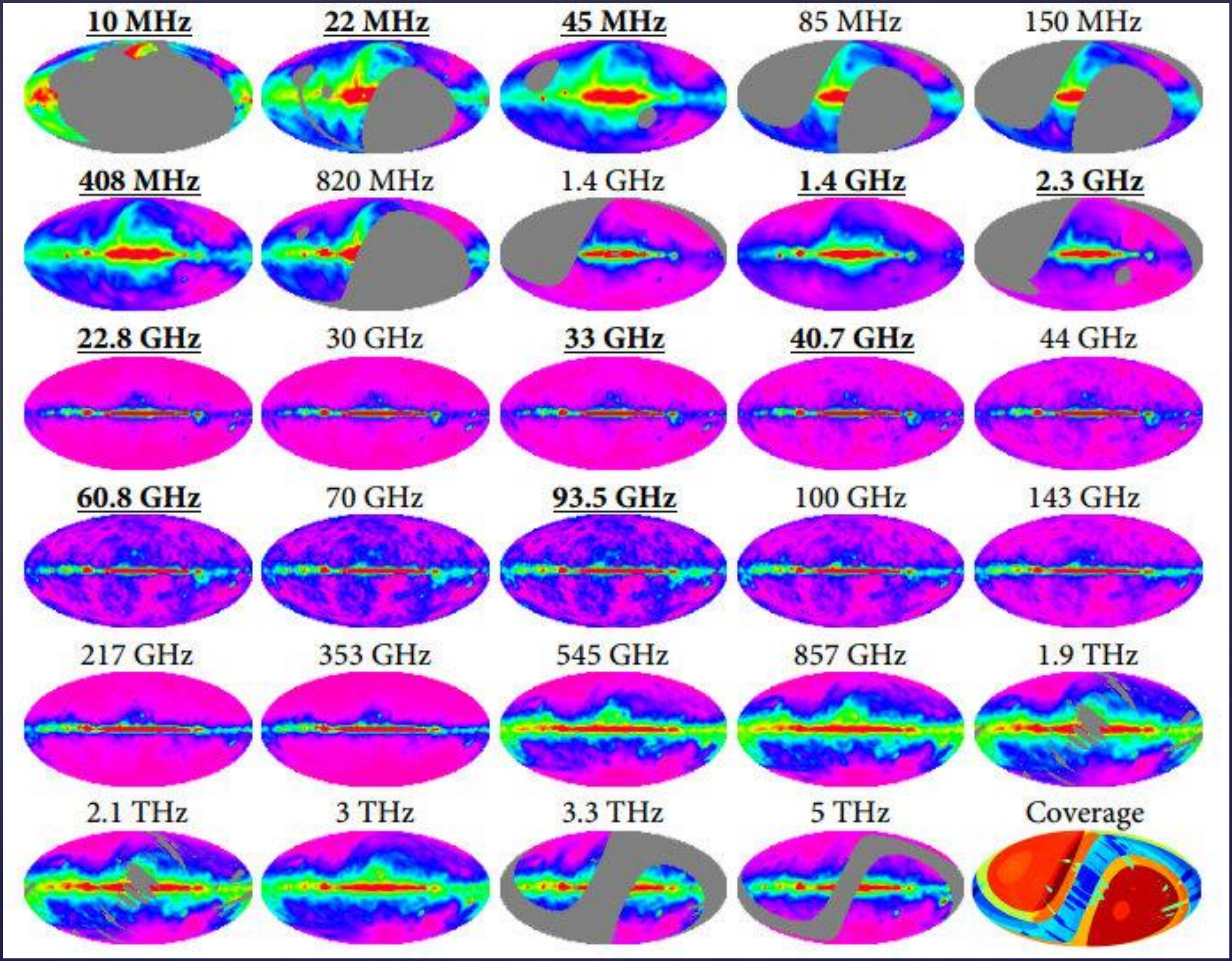

Zheng et al. 2016

LOFAR – Deepest Image

0.8 mJy

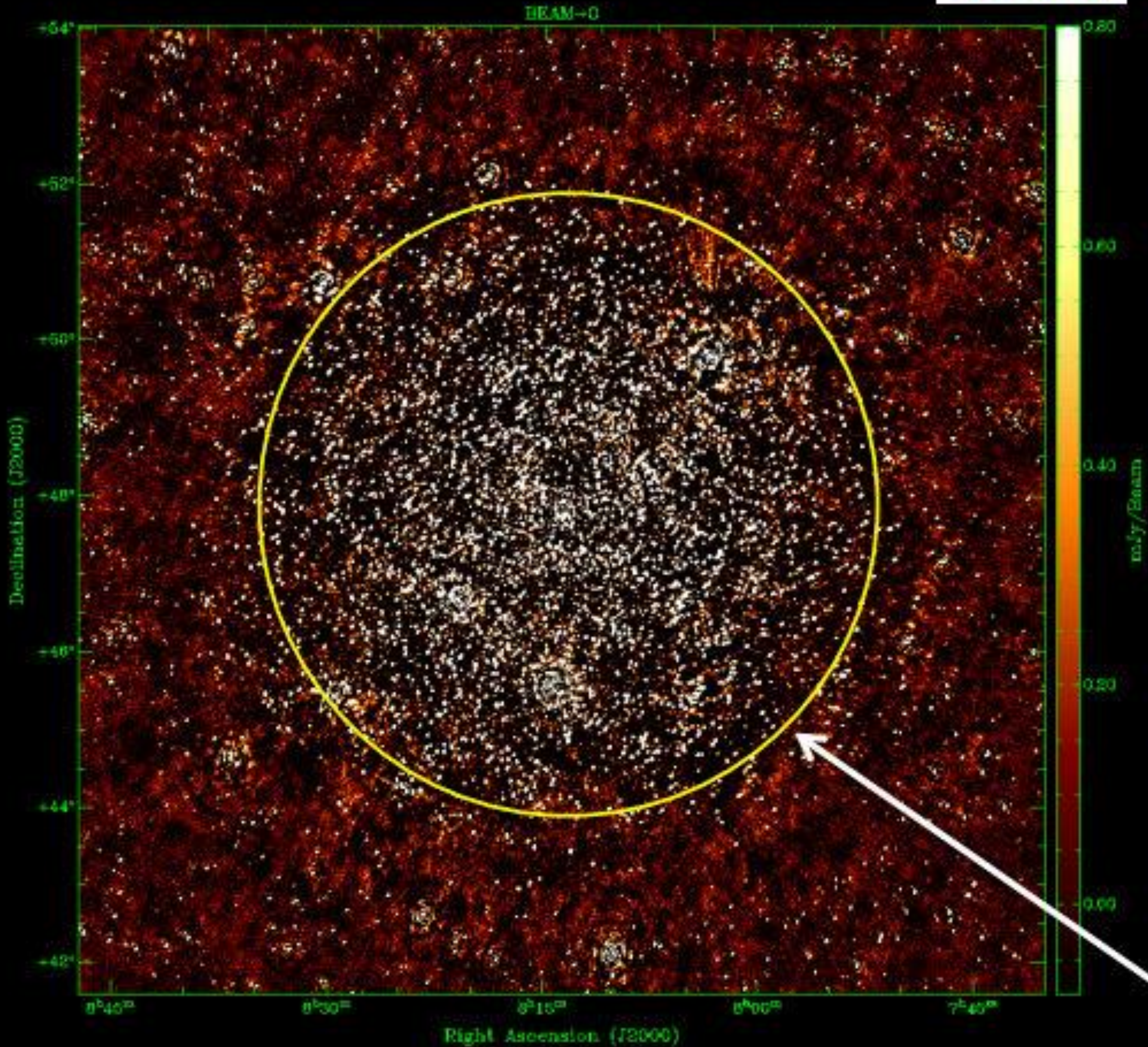

3C196 Field Image

- 145 MHz (~2m)
- 60MHz continuum
- 6 powers of 10

- 32 hours on 3C196 (8 hrs x 4 days)
- Dec 21,12-Feb08,13
- 30λ - 5000λ
- Resolution - 50"
- 12^0 x 12^0 Image

- 'Noise' < 75 μJy
- 3C196 - 79.97 Jy
- **DR: ~ 10^6:1**

Station beam (~8^0)

Pandey 2014

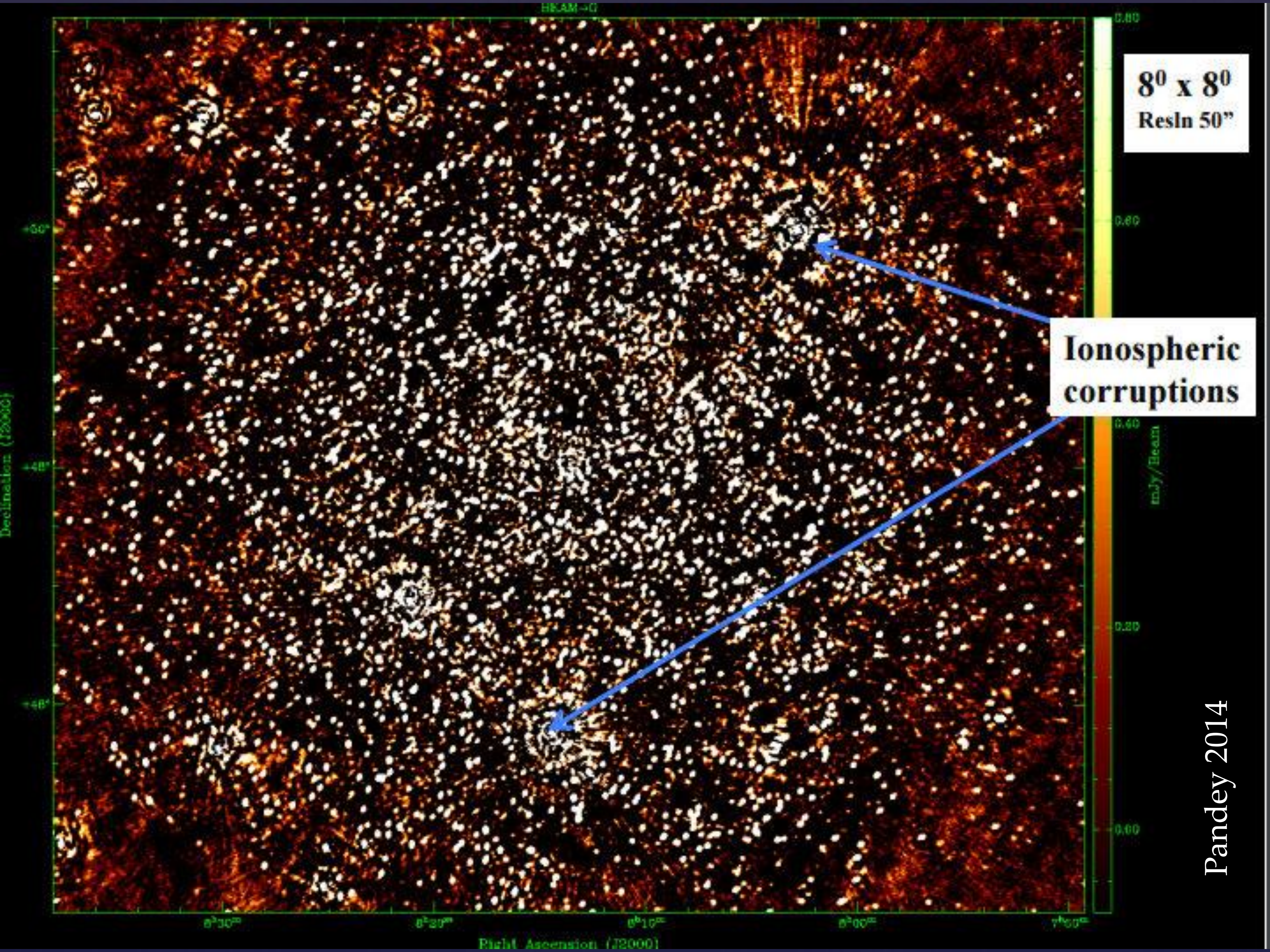

$8^0 \times 8^0$
Resln 50"
Ionospheric corruptions
Pandey 2014
Right Ascension (J2000)
Declination (J2000)
mJy/Beam

Characterize Foregrounds with GMRT – TGSS (ADR)

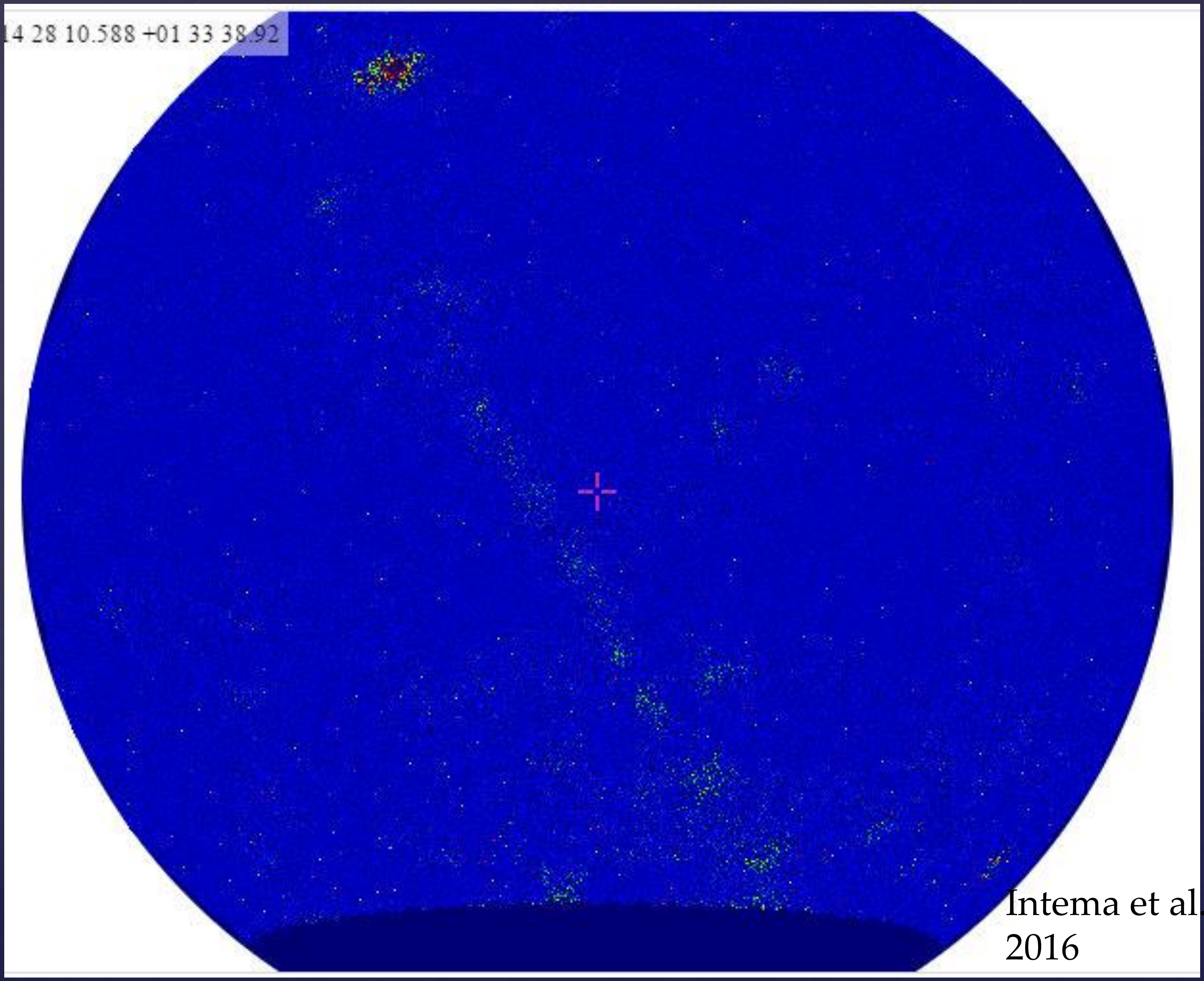

Constraint Foregrounds with GMRT – TGSS (ADR)

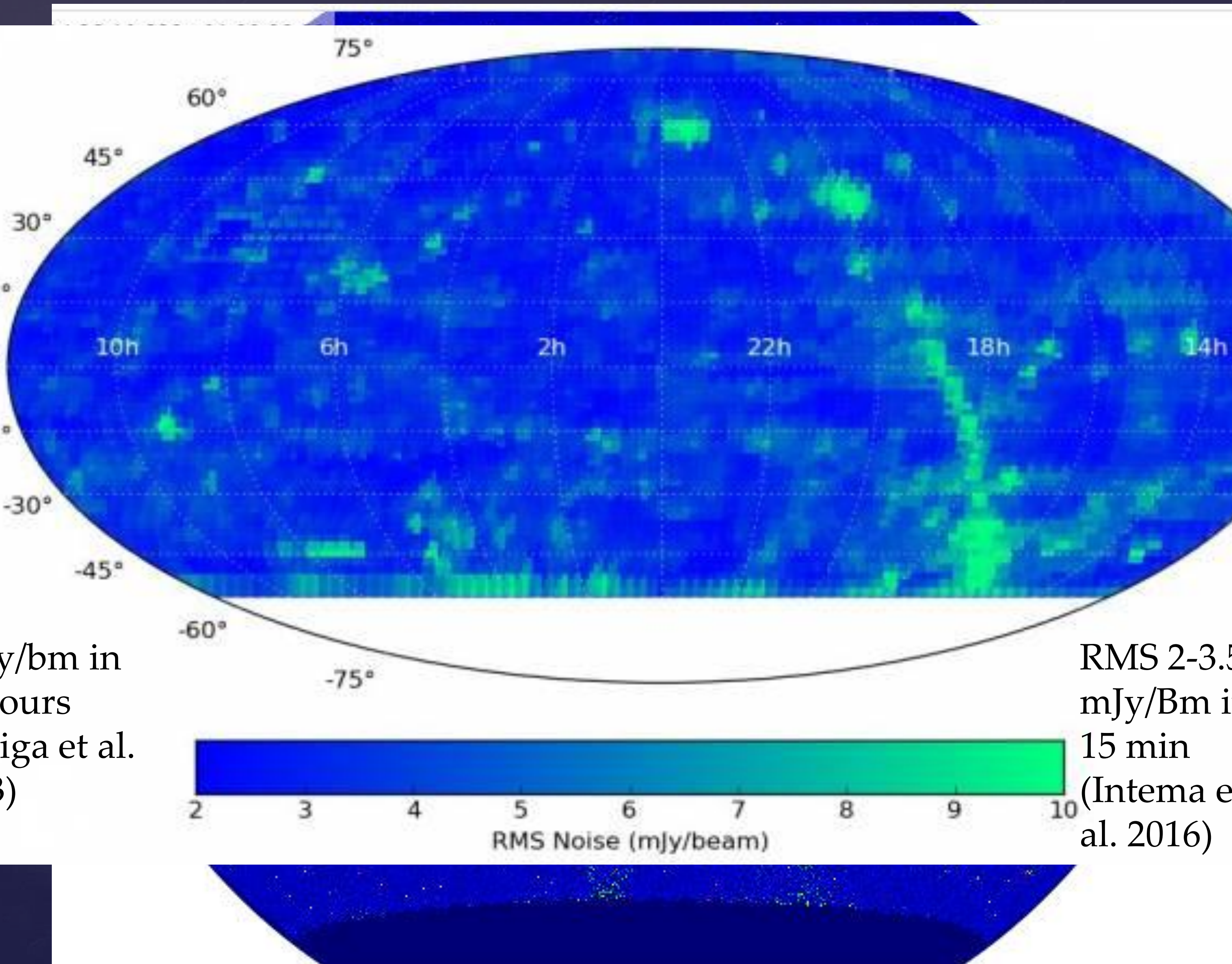

2mJy/bm in 40 hours (Paciga et al. 2013)

RMS 2-3.5 mJy/Bm in 15 min (Intema et al. 2016)

Challenges with Accurate Foreground Models

- Direction Independent Calibration Errors – Datta et al. 2009
- Direction Dependent Calibration Errors – Peeling..
- Primary Beam Calibration
- Ionosphere Calibration
- Polarization Leakage.

Differential Ionospheric Refraction

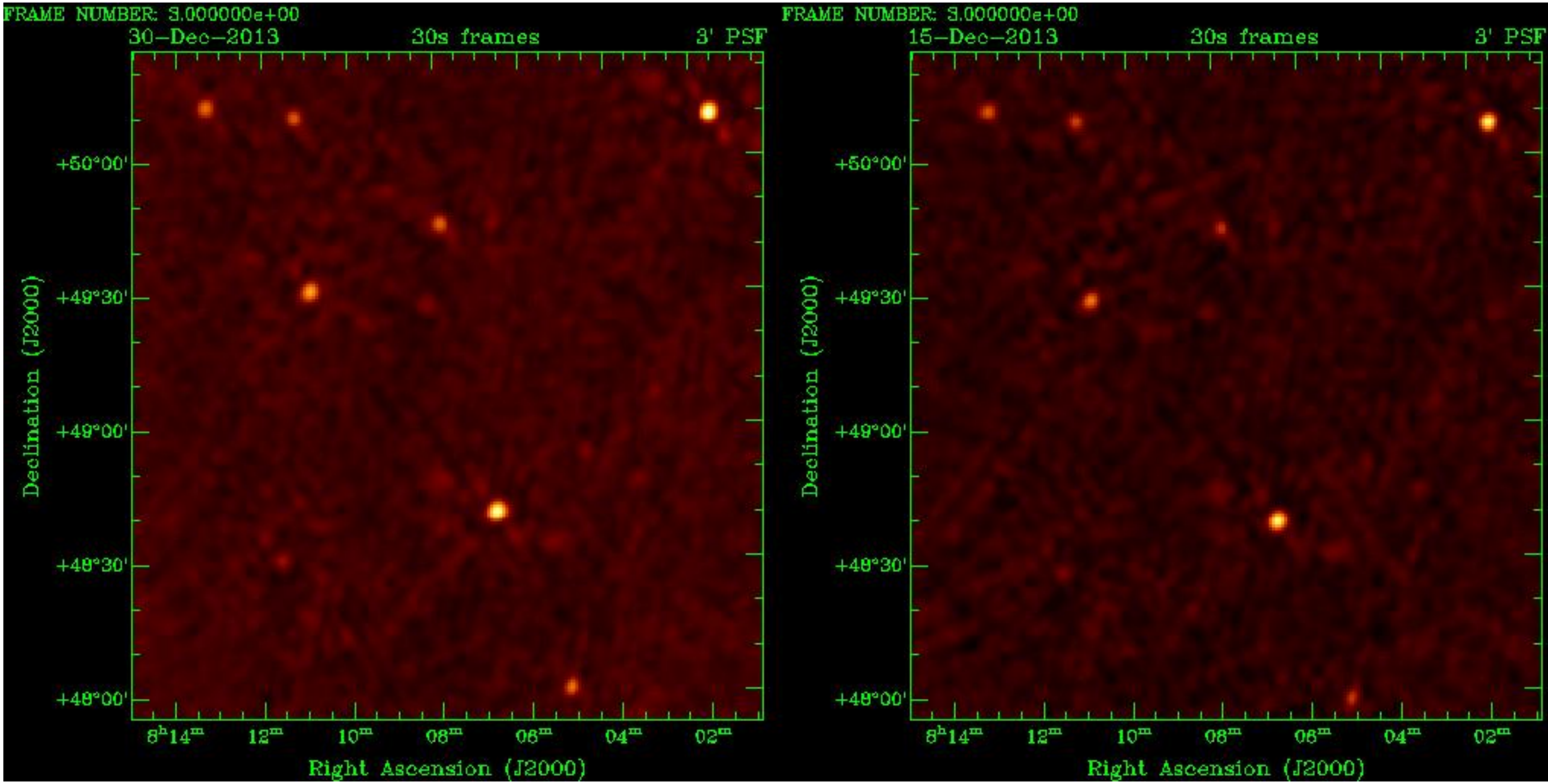

LOFAR

Typical Ionospheric Corruptions

Characteristic	Typical Value (at 100 MHz)	Frequency Scaling
Phase-path Length	-400 meters	ν^{-2}
Phase Change	-840 radians	ν^{-1}
Refraction	1.3 arcminutes	ν^{-2}
Polarization Rotation	6.6 radians*	ν^{-2}
Attenuation	0.01 dB	ν^{-2}

Visibility Equation

- The full equation including the ionospheric term :-

$$V(u,v,w)=\iint I(l,m)\mathrm{e}^{2\pi\iota\left(ul+vm+w\left(\sqrt{1-l^2-m^2}-1\right)-\Phi_{ion}(l,m)\right)}\frac{dl\,dm}{\sqrt{1-l^2-m^2}}$$

- Where

$$\Phi_{ion}(l,m)=\Phi_{ij}(l,m,u,v,t)$$

$$\Phi_{ij}=\Phi_i(\vec{x}_i,t)-\Phi_j(\vec{x}_j,t)$$

$$\vec{x}_i,\vec{x}_j=f(l,m,u,v,t)$$

- Expressed in Taylor series :-

$$\Phi_i(\vec{x}_i)=\Phi_i(\vec{x}_i^o)+\Delta\vec{x}_i\nabla\Phi_i+\frac{(\Delta\vec{x}_i)^2}{2!}\nabla^2\Phi_i+\ldots$$

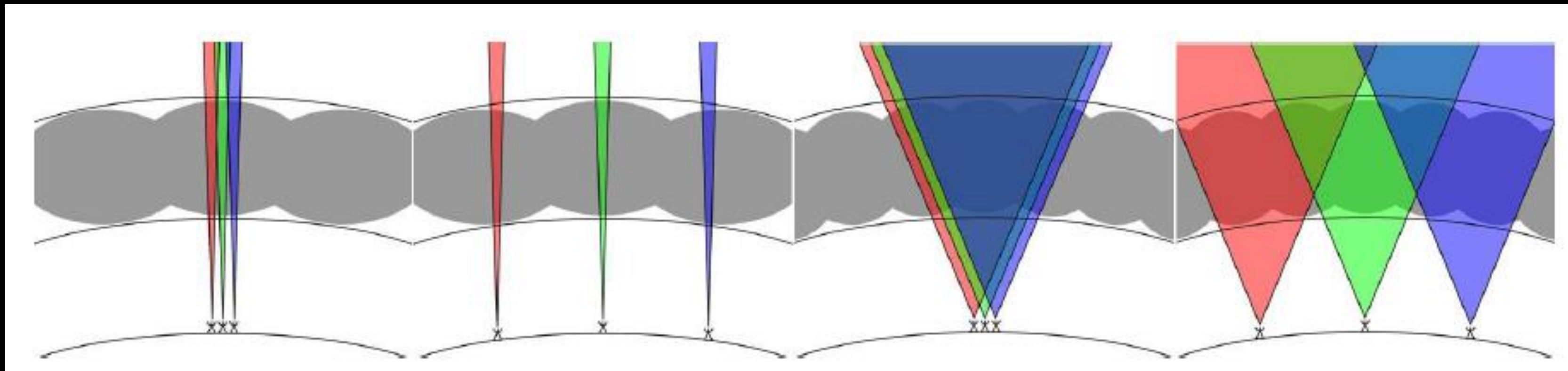

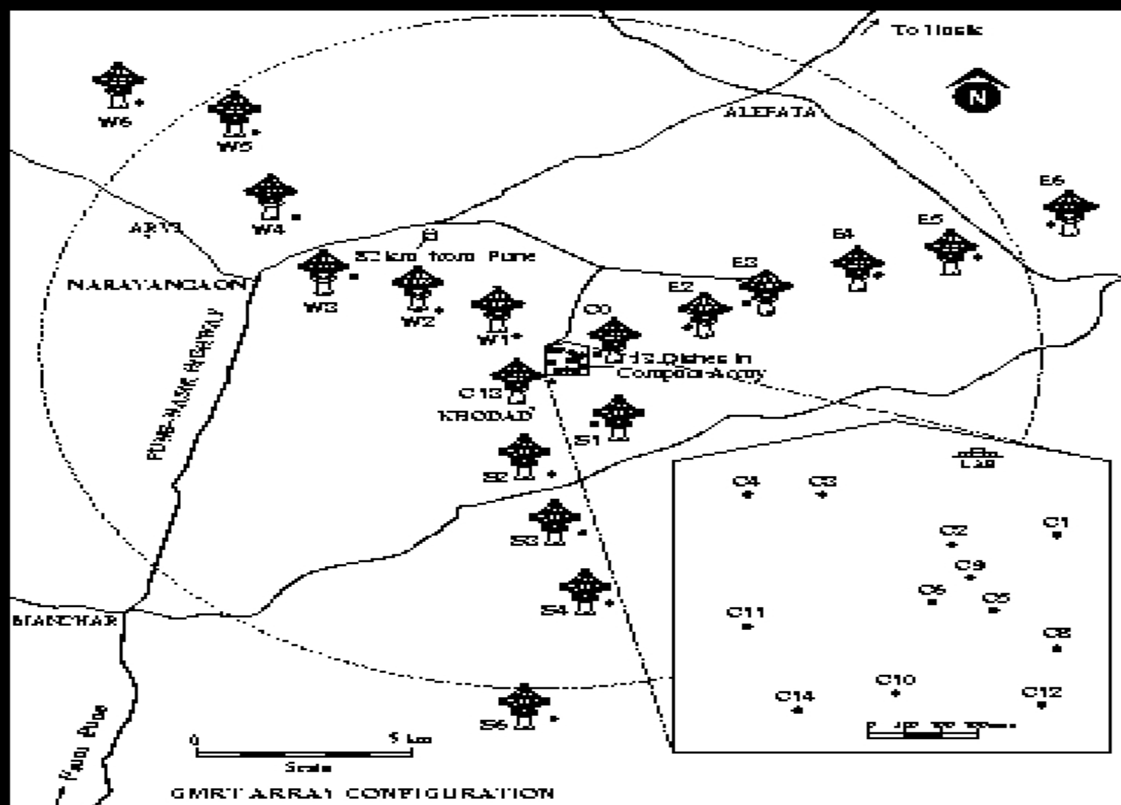

ALEFATA
NARAYANGAON
W6
W5
W4
W3
W2
W1
E6
E5
E4
E3
E2
C0
C13
KHODAD
S1
S2
S3
S4
S6
C4
C3
C2
C1
C9
C6
C5
C11
C8
C10
C14
C12
0
5 km
Scale
GMRT ARRAY CONFIGURATION